Optical properties of thermally vacuum evaporated $AgSbSe_2$ thin films

1998 J. Phys.: Condens. Matter 10 847

(http://iopscience.iop.org/0953-8984/10/4/013)

J. Phys.: Condens. Matter **10** (1998) 847–856. Printed in the UK PII: S0953-8984(98)85990-0

Optical properties of thermally vacuum evaporated $AgSbSe_2$ thin films

H S Soliman†, D Abdel-Hady‡ and E Ibrahim‡

† Ain Shams University, Faculty of Education, Physics Department, Roxy, Cairo, Egypt

‡ Ain Shams University, Faculty of Engineering, Engineering Physics Department, Abassia, Cairo, Egypt

Received 11 July 1997

Abstract. Silver antimony diselenide ($AgSbSe_2$) thin films were prepared by a thermal vacuum evaporation technique onto quartz and glass substrates kept at room temperature (∼300 K). The as-deposited films were amorphous and transformed to a face centred cubic (FCC) polycrystalline nature with the lattice constant $a = 5.797 \pm 0.003$ Å on post-deposition annealing above 423 K for one hour in argon atmosphere. The optical constants (the refractive index n, and the absorption index k) of the films were determined for several samples of different thickness (180 nm–270 nm), using spectrophotometric measurements of the transmittance T and reflectance R at normal incidence in the spectral range 500–2500 nm. These constants were also determined for preannealed films, $T_A = 423$ K (polycrystalline). The obtained values of both n and k were independent of the film thickness within the above-mentioned thickness range. The refractive index data fitted a single-oscillator model with high-frequency dielectric constants increasing from 13 for the amorphous films to 15 for the crystalline films. It was found that the high-frequency dielectric constant ϵ_∞ has the same values as the lattice dielectric constant ϵ_L. The analysis of the spectral behaviour of the absorption coefficient in the intrinsic absorption region revealed the existence of an indirect allowed optical transition with energy gap 1.2 eV for amorphous films and 1.03 eV for the crystalline films, respectively.

1. Introduction

There is now voluminous literature on semiconductor compounds with diamond or related structure (e.g. zinc blende and chalcopyrite types). Much less attention has been given to compounds with structure related to that of NaCl [1]. The ternary semiconductor compounds either in single-crystal form or in thin-film form have received considerable interest owing to their optical and electric properties. The importance of semiconductors in technology rests on the fact that they are used in many applications, such as electronic and optoelectronic devices [2–6]. Very little attention is paid to the compounds of the type $A^IB^VC_2^{VI}$ of which $AgSbSe_2$ is of special interest. Only a few papers dealing with the electronic properties of thin $AgSbSe_2$ films have been published. $AgSbSe_2$ is one of the semiconducting compounds which have the NaCl-type structure [1, 7]. It is particularly disordered with selenium atoms occupying the chlorine sites, while silver and antimony atoms are arranged at random on the sodium sites.

Patel and coworkers [8, 9] have reported the preparation and crystallization of $AgSbSe_2$ films on various substrates. There are only very few data in the literature concerning studies of structural and electrical properties of $AgSbSe_2$films. To our knowledge the optical properties of such films have not been studied before.

0953-8984/98/040847+10$19.50

In this paper, we report the structural properties of $AgSbSe_2$ in a powder form and in a thin-film form, using x-ray and electron diffraction techniques. The optical properties, such as the optical constants n and k, the high-frequency dielectric constant ϵ_∞ and lattice dielectric constant ϵ_L, the absorption coefficient α and the optical energy gap E_g, were determined for $AgSbSe_2$ films as deposited and after annealing. The effect of both annealing temperature and the film thickness on these properties of $AgSbSe_2$ thin films will be also investigated.

2. Experimental techniques

The bulk $AgSbSe_2$ material was prepared by direct fusion of stoichiometric amounts of Ag, Sb and Se (purity 99.999%) in a sealed, evacuated silica tube (10^{-4} Pa). The tube was heated in the following steps:

$$300\ \text{K} \xrightarrow{2\ h} 473\ \text{K} \xrightarrow{2\ h} 910\ \text{K (remaining constant 2 h)}$$
$$\xrightarrow{2\ h\ rocking} 1300\ \text{K (remaining constant 2 h)}$$
$$\xrightarrow{2\ h} 910\ \text{K (remaining 4 h)} \rightarrow 300\ \text{K}$$

with continuous vibrational shaking to ensure homogeneity of the sample. The finely powdered material was analysed by x-ray diffraction (XRD): the resulting pattern was carefully checked for the formation of a homogenous single phase.

$AgSbSe_2$ thin films were prepared by direct thermal evaporation of fine-grained powder from a molybdenum boat with a deposition rate of 3 nm s^{-1} on optically flat precleaned quartz or glass substrates, using a coating unit (Edward 306). The vacuum pressure was maintained at 10^{-4} Pa and the substrates were rotated during the deposition process. The film thickness was monitored by a quartz crystal thickness monitor (Edward, type FTM4) and it was also measured interferometrically [10]. XRD was carried out by a diffractometer (Philips PW 1373) using Cu Kα radiation ($\lambda = 0.1542$ nm) which was Ni filtered. A transmission electron microscope (JEOL type JEM 100 cx), operating at 60 kV with a calibrated resolution 0.4 nm and an attached diffraction stage, was used for the microstructure study.

The transmittance T and reflectance R at normal incidence for $AgSbSe_2$ films were recorded using a UV–VIS–NIR double-beam spectrophotometer 3101 PC (Shimadzu, Japan), attached with a specular reflection stage (V-shape) with incidence angle 5°, in spectral range 500–2500 nm. If I_{ft} and I_q are the intensities of the light passing through the film–quartz system and through the reference quartz, respectively, then [11, 12]

$$T = \frac{I_{ft}}{I_q}(1 - R_q) \tag{1}$$

where R_q is the reflectance of quartz. In addition, if the intensity of light reflected from the sample reaching the detector is I_{fr} and that reflected from the reference Al mirror is I_{Al}, then

$$R = \frac{I_{fr}}{I_{Al}} R_{Al} - T^2 R_q \tag{2}$$

where R_{Al} is the reflectivity of the reference (Al mirror). From the measured T, R and the film thickness t, the values of the refractive index n and absorption index k were computed by a special computer program [13] based on minimizing $(\Delta T)^2$ and $(\Delta R)^2$ simultaneously, where

$$(\Delta T)^2 = |T_{(n,k)} - T_{exp}|^2 \tag{3}$$
$$(\Delta R)^2 = |R_{(n,k)} - R_{exp}|^2 \tag{4}$$

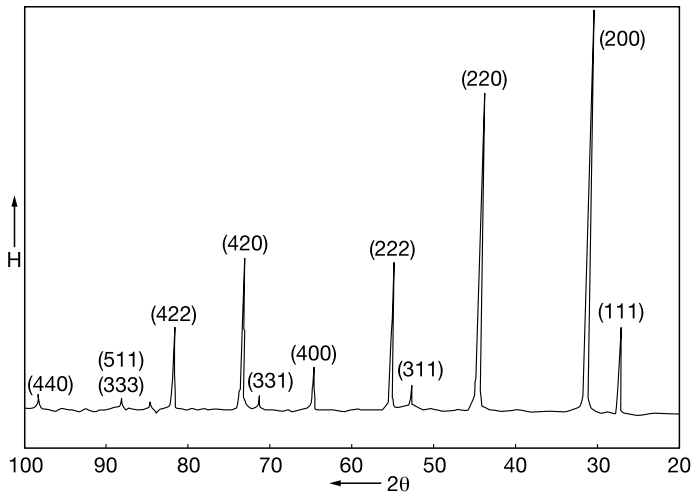

Figure 1. X-ray diffraction pattern of $AgSbSe_2$ in a powder form.

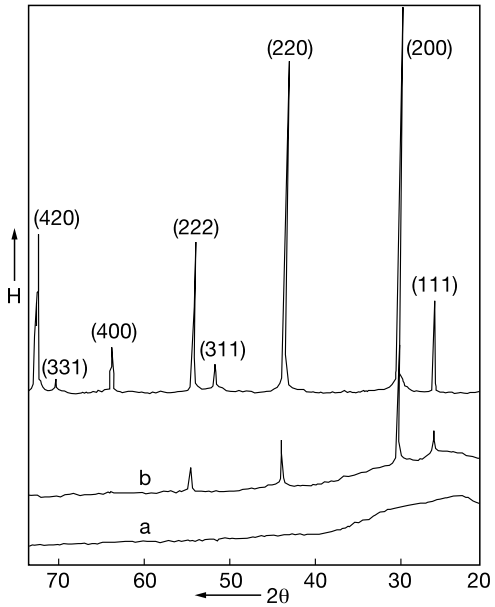

Figure 2. X-ray diffraction patterns of $AgSbSe_2$. a—Amorphous thin film, b—polycrystalline thin film, in comparison with c—powder form.

where T_{exp} and R_{exp} are the experimentally determined values of T and R respectively and $T_{(n,k)}$ and $R_{(n,k)}$ are calculated values of T and R, using the Murmann exact equations [14].

3. Results and discussion

The x-ray diffractogram obtained for $AgSbSe_2$ composition in a powder form is represented in figure 1. Careful analysis of x-ray diffraction pattern indicates the polycrystalline nature

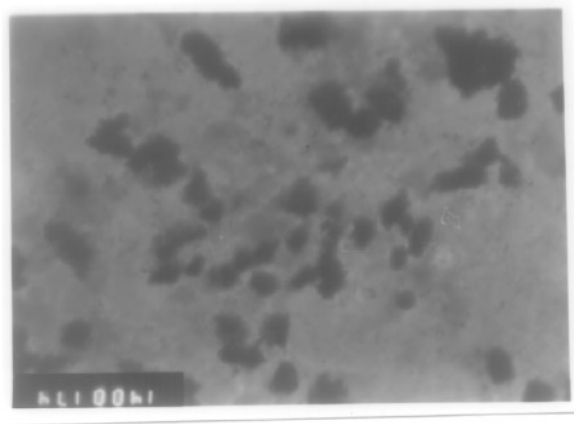

(a)

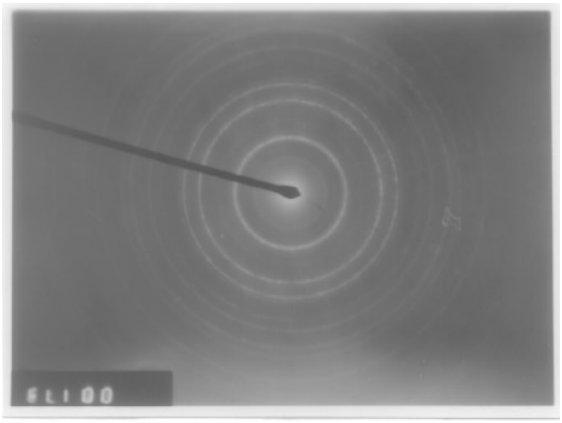

(b)

Figure 3. (a) Transmission electron micrographs of $AgSbSe_2$ films of thickness 50 nm with magnification $\times 3500$. (b) The electron diffraction pattern of the region shown in (a).

of the cubic structure phase with lattice parameter $a = 5.797 \pm 0.003$ Å. The values of peak positions and their corresponding d-values confirm the FCC structure. These values are in agreement with that reported by Geller *et al* [1, 7] and by El-Zahed [15]. Figure 2 illustrates that the typical x-ray diffractograms of the as-deposited (300 K) AgSbSe films of thickness 400 nm are non-crystalline (curve a), while those annealed in argon atmosphere for one hour at $T_A = 423$ K become polycrystalline (curve b). The x-ray diffraction pattern for $AgSbSe_2$ in a powder form is given in the same figure (curve c) for comparison. Analysis of the x-ray diffraction shows that these films have the polycrystalline nature of an FCC phase. The same results were obtained by electron diffraction studies of $AgSbSe_2$ films to check the crystalline nature of films. Figure 3(a) and 3(b) shows the transmission electron micrographs and the corresponding selected area electron diffraction patterns for $AgSbSe_2$ films of thickness 50 nm annealed in argon atmosphere at temperature $T_A = 423$ K for an hour.

Since the as-deposited $AgSbSe_2$ films are non-crystalline, while the preannealed films have a polycrystalline nature, it was interesting to investigate the optical properties of $AgSbSe_2$ films in both cases, i.e. for as-deposited and annealed films.

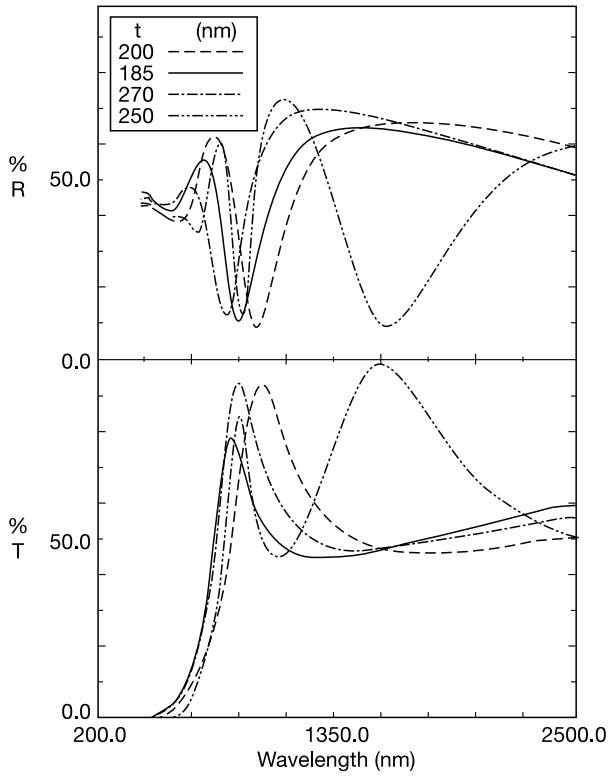

Figure 4. The spectral distribution of the $T_{(\lambda)}$ and $R_{(\lambda)}$ for $AgSbSe_2$ thin films of different film thicknesses measured in the spectral range of 500–2500 nm for as-deposited samples.

The spectral behaviour of the normal incidence transmittance $T_{(\lambda)}$ and reflectance $R_{(\lambda)}$ for as-deposited non-crystalline $AgSbSe_2$ films and for the same films after post-deposition annealing at $T_A = 423$ K in an argon atmosphere for one hour (i.e. for crystalline $AgSbSe_2$ films) in the wavelength range 500–2500 nm are shown in figures 4 and 5 respectively. At long wavelengths in the transmission region $T + R = 1$, which indicates that the investigated films become transparent and homogenous on the one hand and that no scattering or absorption of light exists on the other.

The refractive and absorption indices n and k of $AgSbSe_2$ films were determined from the absolute values of the measured transmittance and reflectance of the quartz substrate as given by equations (1) and (2). The determined values of n and k were computed via Muramann's exact equations as mentioned above. Figures 6 and 7 represent the two dependences $n(\lambda)$ and $k(\lambda)$ for amorphous (curves a) and polycrystalline (curves b) $AgSbSe_2$ films. From these figures the following can be concluded.

(i) Both n and k are practically independent of film thickness in the thickness range 185–270 nm.

(ii) The discrepancy in both n and k can be attributed to the experimental errors in T, R and film thickness t.

(iii) The optical constants n and k were slightly affected by the annealing temperature.

The values of n and k shown in figures 6 and 7 represent the average values determined for films of different thickness. The high-frequency dielectric properties can be attributed

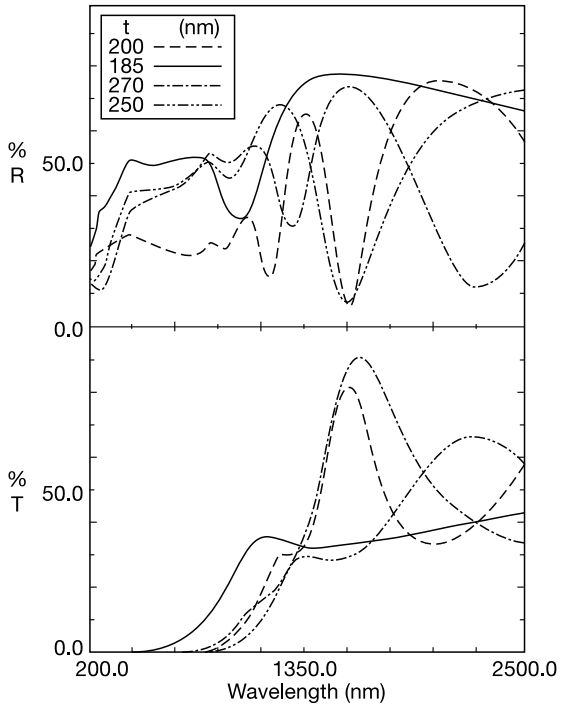

Figure 5. The spectral distributions of $T_{(\lambda)}$ and $R_{(\lambda)}$ for $AgSbSe_2$ thin films of different thicknesses measured in the spectral range of 500 nm to 2500 nm for samples annealed at 423 K for one hour in argon atmosphere.

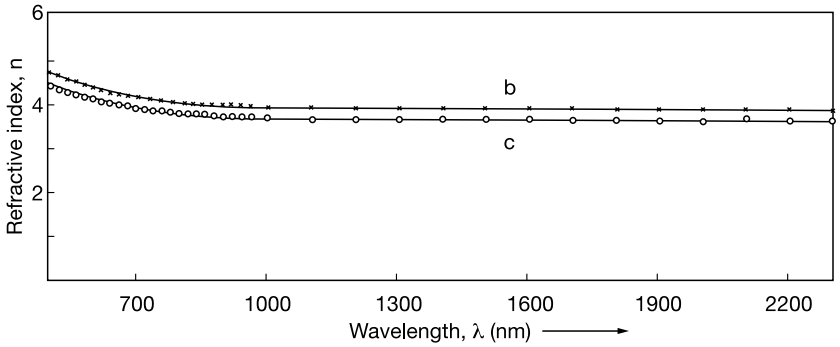

Figure 6. The spectral distributions of $n(\lambda)$ of $AgSbSe_2$ thin films (a) for as-deposited samples and (b) for samples annealed at 423 K for one hour in argon atmosphere.

to a simple classical single oscillator, so the following relation can be used [16, 17]:

$$\frac{n_\infty^2 - 1}{n^2 - 1} = 1 - \left(\frac{\lambda}{\lambda_0}\right)^2 \tag{5}$$

where n_∞ is the refractive index of an empty lattice at an infinite frequency and λ_0 is an average oscillator position. Plotting $[n^2 - 1]^{-1}$ versus λ^{-2} fits a straight line at longer wavelengths (figure 8) for the amorphous (curve a) and polycrystalline (curve b) $AgSbSe_2$ films. Extrapolating these straight lines yields $\epsilon_\infty = n_\infty^2$ equal to 13 and 15 for the

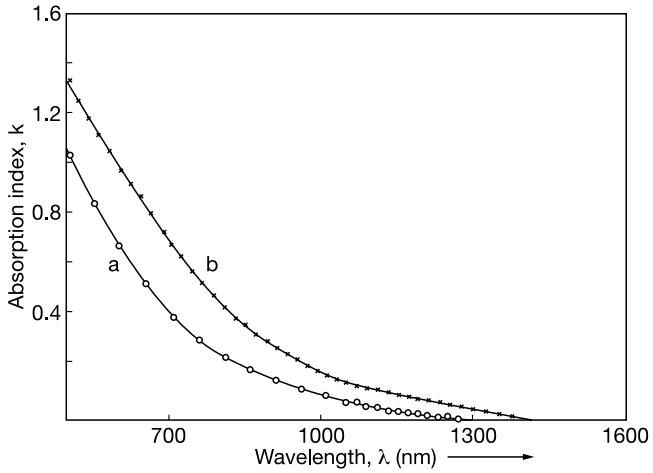

Figure 7. The spectral distribution of $k(\lambda)$ of $AgSbSe_2$ thin films, (a) for as-deposited samples and (b) for samples annealed at 423 K for one hour in argon atmosphere.

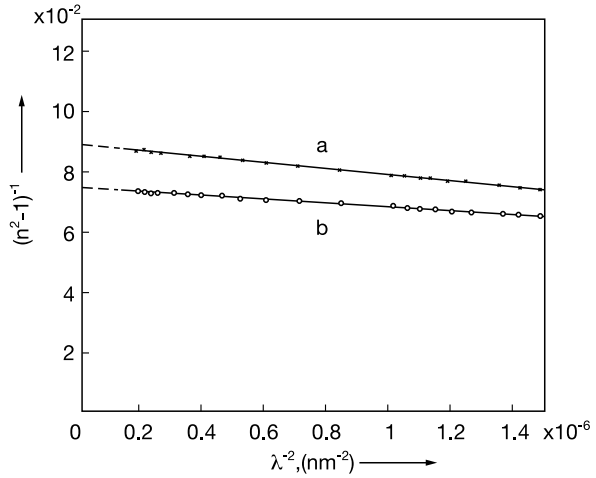

Figure 8. The relation between $[n^2 - 1]^{-1}$ and λ^{-2} for $AgSbSe_2$ thin films (a) for as-deposited samples and (b) for samples annealed at 423 K for one hour in argon atmosphere.

amorphous and crystalline $AgSbSe_2$ films respectively. The real dielectric constant can be represented by the following relation:

$$\epsilon_1 = \epsilon_L - B\lambda^2 \tag{6}$$

where ϵ_L is the lattice dielectric constant and $\epsilon_1 = n^2 - k^2$. A shown in figure 9, the above-mentioned relation is represented by a straight line (a) for amorphous and (b) for polycrystalline $AgSbSe_2$ films. By extrapolation of these lines toward slower values of λ^2, the point of interception of the ordinate at $\lambda^2 = 0$ yields $\epsilon_L = 13$ for amorphous (curve a) and 15 for crystalline (curve b) $AgSbSe_2$ films respectively.

The spectral behaviour of the absorption coefficient ($\alpha = 4\pi k/\lambda$) shows that the absorption edge shifts to the lower-energy side after annealing the as-deposited films at

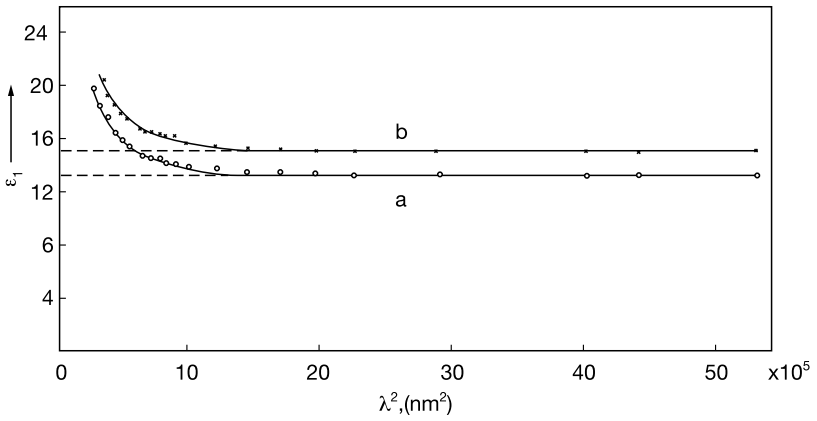

Figure 9. Variation of the real dielectric constant (ϵ_1) as a function of λ^2 for $AgSbSe_2$ thin films (a) for as-deposited samples and (b) for samples annealed at 423 K for one hour in argon atmosphere.

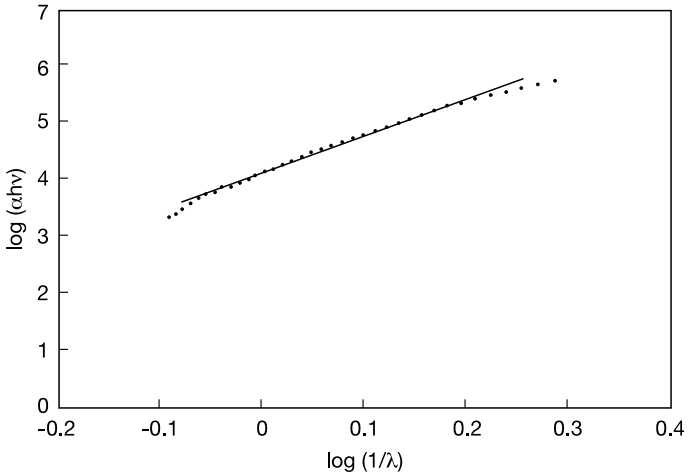

Figure 10. The dependence of $\log(\alpha h\nu)$ on $\log(1/\lambda)$ for the as-deposited $AgSbSe_2$ thin films.

423 K for one hour. The intrinsic absorption edge was examined using the equation [18]

$$\alpha h\nu = A(h\nu - E_g)^x. \tag{7}$$

$x = \frac{1}{2}$ and 2 for direct and indirect allowed optical transitions respectively. In order to know whether there is one type of optical transition or more that can exist in $AgSbSe_2$ thin amorphous films, a graphical representation of $\log(\alpha h\nu)$ against $\log(1/\lambda)$ must be carried out. As shown in figure 10 this relation indicates the existence of one type of optical transition. Figure 11 represent both $(\alpha h\nu)^2 = f(h\nu)$ and $(\alpha h\nu)^{1/2} = g(h\nu)$ for $AgSbSe_2$ thin amorphous films. It is obvious that the second relation yields a straight line indicating the existence of indirect optical transition with an energy gap $E_g^d = 1.2$ eV. Figure 12 illustrates both the above relations for polycrystalline $AgSbSe_2$ films: the linearity of the second relation indicates the existence of allowed indirect optical transition with an energy gap $E_g^d = 1.03$ eV.

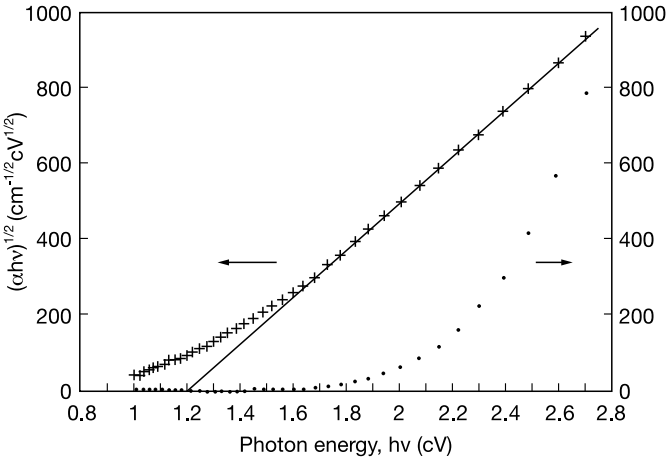

Figure 11. The dependence of $(\alpha h\nu)^2$ and $(\alpha h\nu)^{1/2}$ on photon energy $(h\nu)$ for the as-deposited $AgSbSe_2$ thin films.

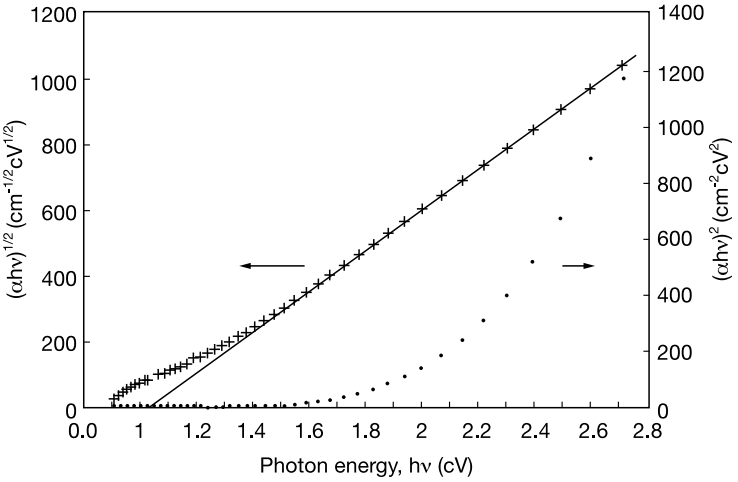

Figure 12. The dependence of $(\alpha h\nu)^2$ and $(\alpha h\nu)^{1/2}$ on photon energy $(h\nu)$ for the $AgSbSe_2$ thin films annealed at 423 K for one hour in argon atmosphere.

4. Conclusion

In this research the original material of $AgSbSe_2$, either in powder or in a thin-film form after being annealed in argon for one hour at 423 K, has polycrystalline nature corresponding to an FCC phase with lattice parameter $a = 5.797 \pm 0.003$ Å. However, $AgSbSe_2$ thin films, as deposited, have amorphous nature.

The optical constants determined for amorphous and crystalline $AgSbSe_2$ films were found to be independent of the film thickness in the thickness range 185–270 nm. The high-frequency dielectric constant ϵ_∞ of amorphous $AgSbSe_2$ films is found to be 13 and increased to 15 for polycrystalline films. The same values were arrived at for lattice dielectric constant ϵ_L.

The energy gap of the existing allowed nondirect optical transition in amorphous $AgSbSe_2$ films is found to be 1.2 eV and it is decreased to 1.03 eV for polycrystalline films.

References

[1] Geller S and Wernick J H 1959 *Acta Crystallogr*. **12** 46
[2] Kunoka A and Sakai Y 1968 *Japan. J. Appl. Phys.* 1138
[3] Sreedhar A K, Sharma B L and Rurohit R K 1970 *Phys. Status Solidi* a **3** K217
Sreedhar A K, Sharma B L and Rurohit R K 1969 *IEEE Trans. Electron Devices* **ED-16** 309
[4] Goodwin A R and Selway P R 1970 *IEEE J. Quantum Electron.* **QE-6** 285
[5] Castellano A 1986 *J. Appl. Phys. Lett.* **48** 298
[6] Van O-p-dorp C and Vrakking J 1967 *Solid State Electron.* **10** 955
[7] Wernick J H, Geller S and Benson K E 1958 *J. Phys. Chem. Solids* **4** 154
[8] Patel A R, Lakshminaray D and Rao K V 1982 *Thin Solid Films* **94** 51
[9] Patel A R and Lakshminaray D 1982 *Thin Solid Films* **98** 59
[10] Tolansky S 1970 *Multiple-beam Interference Microscopy of Metals* (London: Academic) p 55
[11] Agiev L A and Shklyareveskii I N 1978 *J. Percale Spekt.* **76** 380
[12] Shklyareveskii I N, Kornveeva T I and Zozula K N 1969 *Opt. Spectrosc.* **27** 174
[13] Soliman H S, El-kadry N, Gamjoum O, El-Nahass M M and Darwish H B 1988 *Indian J. Opt.* **17** 46
[14] Liddell H M 1981 *Computer-aided Techniques for the Design of Multilayer Filters* (Bristol: Hilger) p 118
[15] El-Zahad H 1994 *Thin Solid Films* **238** 104
[16] Moss T S, Burrell G J and Ellis B 1973 *Semiconductor Optoelectronics* (London: Butterworths) p 23
[17] DiDomenico M and Wemple S H 1969 *J. Appl. Phys.* **40** 720
[18] Bardeen J, Blatt F J and Hall L H 1956 *Proc. Photoconductivity Conf.* ed R Breckenridge *et al* (New York: Wiley)